

Figure S1. Denervation reduces fucosylation of intestinal epithelium. Related to Figure 1.

(A-B) Representative whole mount microscopy (A) and immunofluorescence image (B) of co-staining epithelium and enteric neurons in the mouse ileum. Scale bar, 50 μm .

(C) Anatomical diagram for subdiaphragmatic truncal vagotomy.

(D) A heat map depicts expression levels of the major changes in genes including glycosylation.

(E) Real-time PCR analysis of Fut2 mRNA in IECs of duodenum and Jejunum from Sham mice and VGx mice. Mean \pm SEM; n = 5, *p < 0.05.

(F) Representative plots of FACS and summary graphs of the percentage of UEA-1 stained IECs of duodenum and Jejunum from Sham and VGx mice. Mean \pm SEM; n = 6-7, *p < 0.05.

(G) Immunofluorescence sections (i) and quantification (ii) of Muc2 (green) and UEA-1 (red) co-staining of ileum in Sham mice or VGx mice. Scale bar, 50 μm .

(H) Real-time PCR analysis of Fut1 and Fut2 mRNA in colonic IECs from Sham mice and VGx mice. Mean \pm SEM; n = 5, ns, not significant.

(I) Immunofluorescence sections of UEA-1 staining of colon in Sham mice or VGx mice. Scale bar, 50 μm .

(J) Representative plots of FACS and summary graphs of the percentage of UEA-1 stained IECs of large intestine (LI) from Sham and VGx mice. Mean \pm SEM; n = 6-7, ns, not significant.

(K) Pattern of fucosylation modification in the IECs from larger intestine from Sham mice or VGx mice. Coomassie blue staining (left) was used to show total protein input, UEA-1 staining blot (middle) and quantification (right) were used to show fucosylated-protein.

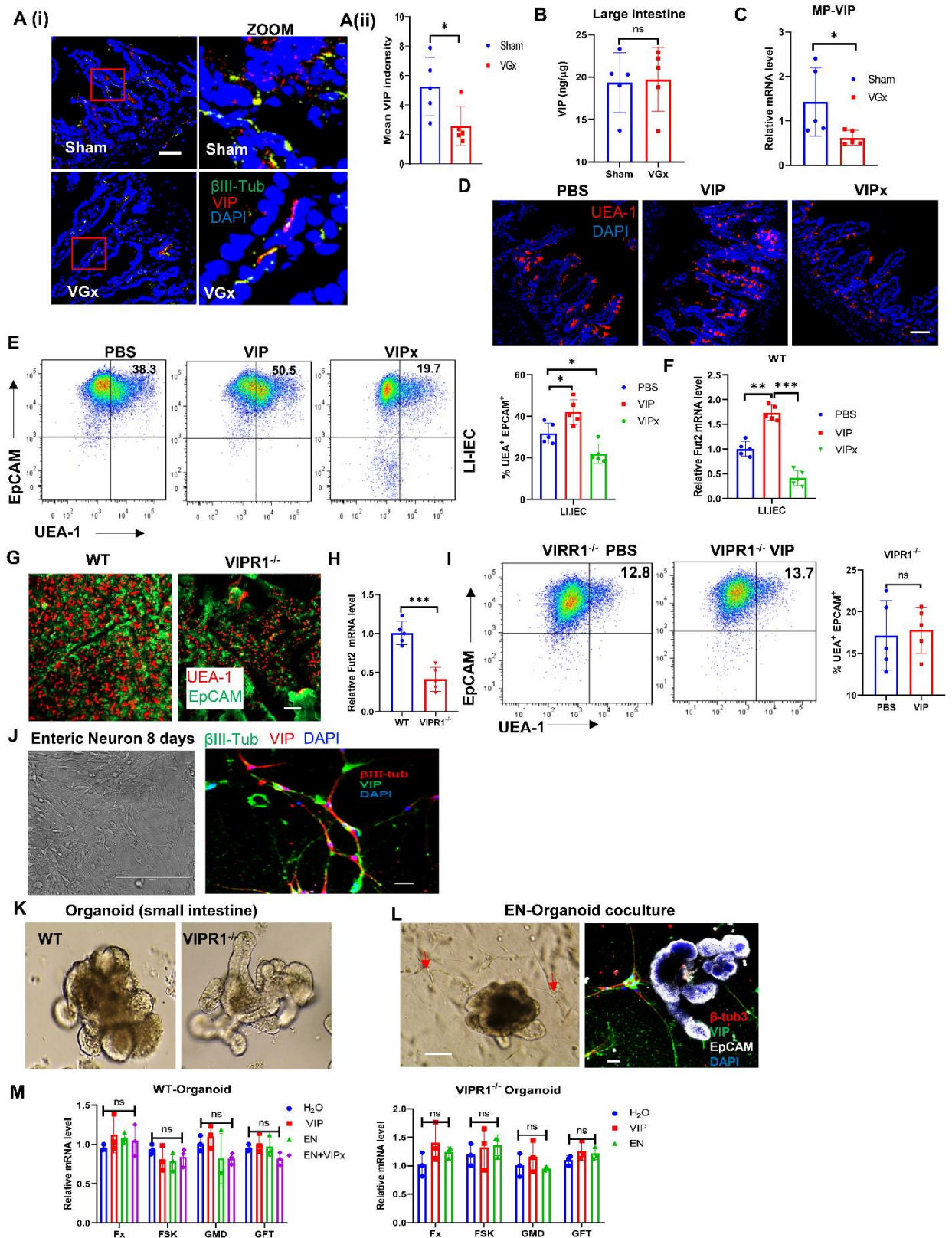


Figure S2 VIP-VIPR1 signaling regulates epithelial fucosylation. Related to Figure 2.

(A) Representative immunofluorescence image (i) and image quantification (ii) of VIP enteric neuron (EN) by markers staining with β III-Tubulin (β III-Tub, green), VIP (red), and DAPI (blue) in the ileum of Sham mice or VGx mice with chow diet. Scale bar, 50 μ m.

(B) EIA measurement of concentration of VIP in the colon of Sham mice or VGx mice. n = 5 mice, Mean \pm SEM; ns: not significant.

(C) Real-time PCR analysis of the VIP mRNA expression in myenteric plexus (MP) of the ileum from Sham mice or VGx mice.

(D) Immunofluorescence section of UEA-1 and DAPI staining of ileum in WT mice 12 h after injection with PBS, VIP (6 μ g/mice) or VIPx (100 μ g/mice). Data are representative of at least 5 mice per condition. Scale bar, 50 μ m.

(E) Representative plots of FACS and summary graphs of the percentage of UEA-1 stained IECs of colon in WT mice after injection with PBS, VIP or VIPx.

(F) Real-time PCR analysis of Fut2 expression in IECs of colon in WT mice 12 h after injection with PBS, VIP or VIPx.

(G) Whole mount microscopy of UEA-1 staining of colon in WT mice or VIPR1^{-/-} mice. Scale bar, 50 μ m.

(H) Real-time PCR analysis of fut2 gene expression in IECs derived from WT mice or VIPR1^{-/-} mice.

(I) Representative plots of FACS and summary graphs of the percentage of UEA-1 stained IECs from VIPR1^{-/-} mice 12h after injection with PBS or VIP.

Data (C, F, H) are from at least two independent experiments and representative of at least 5 mice per condition. Mean \pm SEM; *p < 0.05, **p < 0.01, ***p < 0.01, ns: no significant.

(J) Representative phase-contrast (left, scale bar, 200 μ m), and immunofluorescent (right, scale bar, 50 μ m) micrographs of primary enteric neurons cultured from small intestinal myenteric plexuses of 8-week-old mouse. After 8 days in culture, cells were fixed and stained with β III-Tub (green), VIP (red) and DAPI. Representative of 2 or more fields in 3 independent cultures.

(K) Brightfield image of a mature (day 9) mouse intestinal organoids derived from WT mice or VIPR1^{-/-} mice. The central lumen is surrounded by an epithelial monolayer with budding crypt-like domains. Scale bar, 50 μ m.

(L) Representative phase-contrast (left) and immunofluorescent (right) micrographs of primary enteric neurons (EN) co-cultured with intestinal organoids. After 5 days in co-culture, cells were fixed and stained with VIP (green), β III-Tub (red), EpCAM (grey) and DAPI. Representative of 2 or more fields in 3 independent cultures. Scale bar, 50 μ m.

(M) Real-time PCR analysis of indicated genes expression involved in fucosylation biosynthesis in intestinal organoids from WT mice (left) or from VIPR1^{-/-} mice (right). Intestinal organoids were cultured with/without intestinal MP neurons for 5 days, 1 μ M of VIPx was added into organoid cultures 24 h before sample collection as indicated. Fx, GDP-4-keto-6-deoxymannose-3,5-epimerase-4-reductase; FSK, fucose kinase; GMD, GDP-mannose 4,6-dehydratase; GFT, GDP-Fucose Transporter. Representative of three independent cultures. Mean \pm SEM; n = 5, ns: not significant.

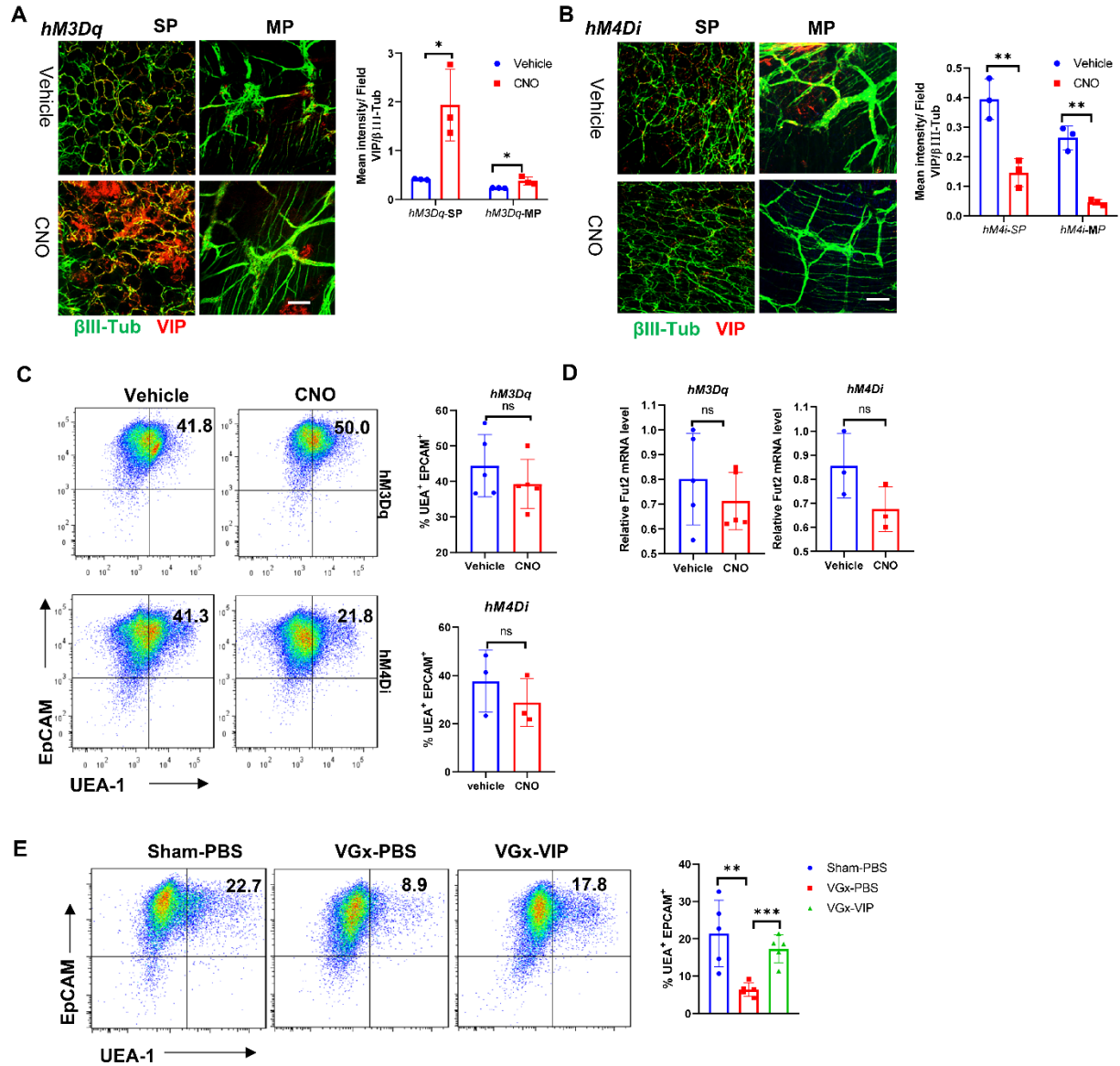


Figure S3 Effect of VIPergic neuronal modulation with DREADDs on IECs Fucosylation. Related to Figure 2.

(A-B) Representative immunofluorescence staining and quantification of VIPergic neurons in both submucosa plexus and myenteric plexus with β III-Tub (green), VIP (red) from ileum of vehicle or CNO injection *Vip^{IRE5-cre}hM3Dq^{fl/+}* mice (activating DREADD, B) or *Vip^{IRE5-cre}hM4Di^{fl/fl}* mice (inhibiting DREADD, C). Scale bar, 50 μ m.

(C) Representative plots of FACS and summary graphs of the percentage of UEA-1 stained colonic IECs from *Vip^{IRE5-cre}hM3Dq^{fl/+}* mice or *Vip^{IRE5-cre}hM4Di^{fl/fl}* 36 h after treatment with vehicle or CNO. n = 3-5.

(D) Real-time PCR analysis of Fut2 expression in colonic IECs from *Vip^{IRE5-cre}hM3Dq^{fl/+}* mice or *Vip^{IRE5-cre}hM4Di^{fl/fl}* 24 h after treatment with vehicle or CNO. n = 3-5.

(E) Representative plots of FACS and summary graphs of the percentage of UEA-1 stained IECs from sham mice or VGx mice 12 h after the last injection with PBS or VIP (6 µg/mice).

Representative of 3 independent experiments. Mean ± SEM; ns: not significant.

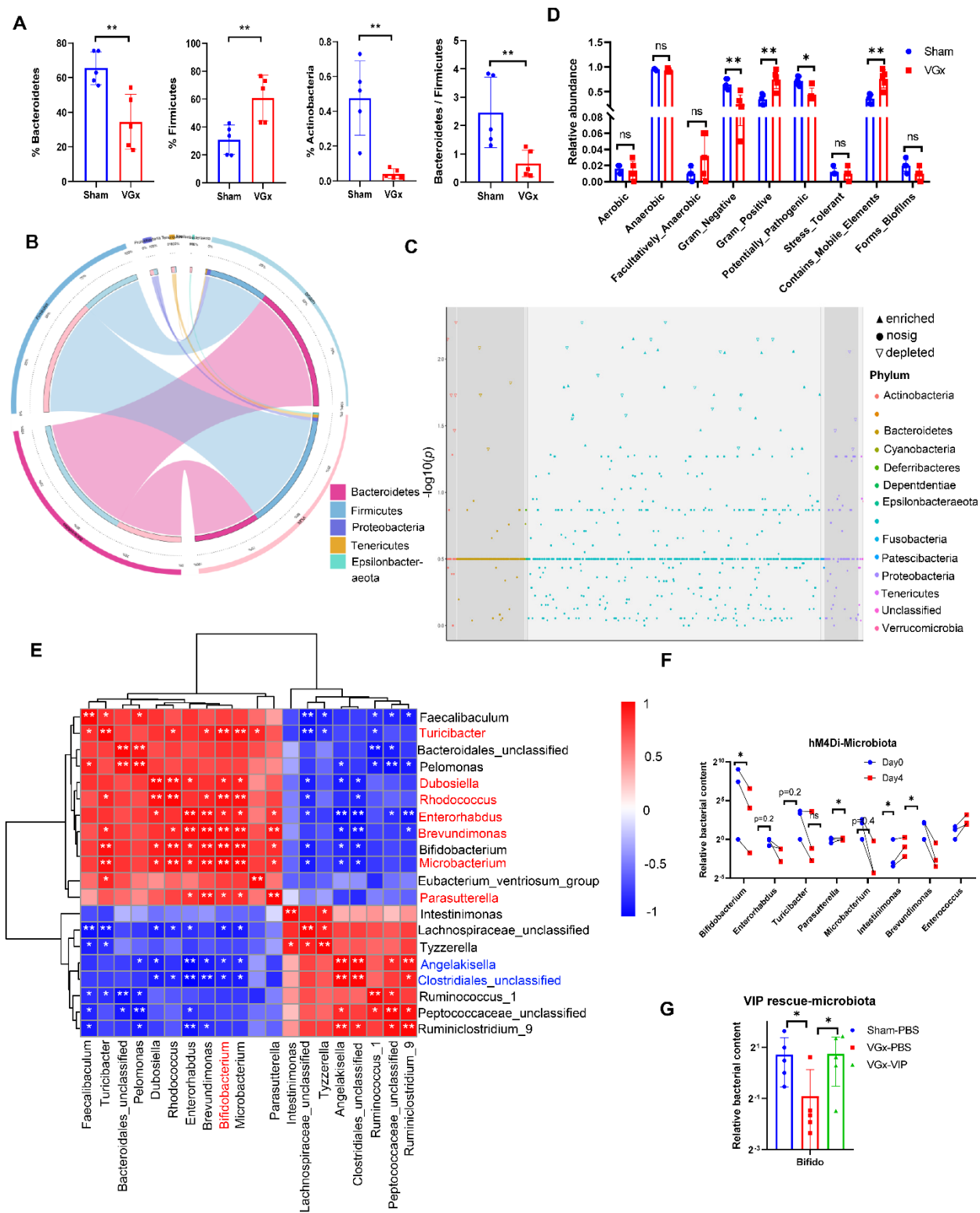


Figure S4. Disturbance of enteric neuron regulates the composition of gut microbiota.

Related to Figure 4.

(A) Bar graph of abundance of microbiota at the phylum level in the Sham and VGx samples determined by 16S rRNA sequencing. Data were shown as mean \pm SEM; n = 5, **p < 0.01.

(B) The circos plot displays relative abundance of bacterial phyla within Sham and VGx samples. The abundance of each phylum (assigned a specific color) is directly proportional to the width of each ribbon connecting bacterial taxa to its respective sample. The outer circle represents the number of 16S rRNA sequences assigned to a given taxa in a given sample.

(C) The manhattan plot relative bacterial abundance at phylum level within Sham and VGx samples. Each phylum is assigned a specific color as indicated. Significantly changed bacterial phylum were indicated with a solid triangle (higher in Sham samples) and an unfilled triangle (higher in VGx samples). The threshold of the p-value was indicated with red dashed line.

(D) Bar graph showing the abundance of microbiota with functional clustering in the Sham and VGx samples. Data were analyzed by BugBase software and shown as mean \pm SEM; n = 5, *p < 0.05, **p < 0.01, ns, not significant.

(E) The Spearman correlation heatmap graphically represents the correlation between the top 20 most changed bacterial genera. R values (value of coefficient) are shown in different colors as indicated in the figure. * p < 0.05; ** p < 0.01.

(F) Relative abundance of bacterial genera in fecal samples from *Vip^{IRE5-cre}hM4Di^{fl/fl}* day 0 and day 4 after treatment with CNO determined by real-time PCR. *Vip^{IRE5-cre}hM4Di^{fl/fl}* mice were treated with CNO (1 mg per kg bodyweight (mg/kg) intraperitoneally daily for 4 days.

(G) Relative levels of *Bifidobacterium* in the lumen in sham mice or VGx mice 12h after the last injection with PBS or VIP (6 μ g/mice) assessed by real-time PCR. (F-G) Representative of 3 independent experiments. Mean \pm SEM; ns: not significant.

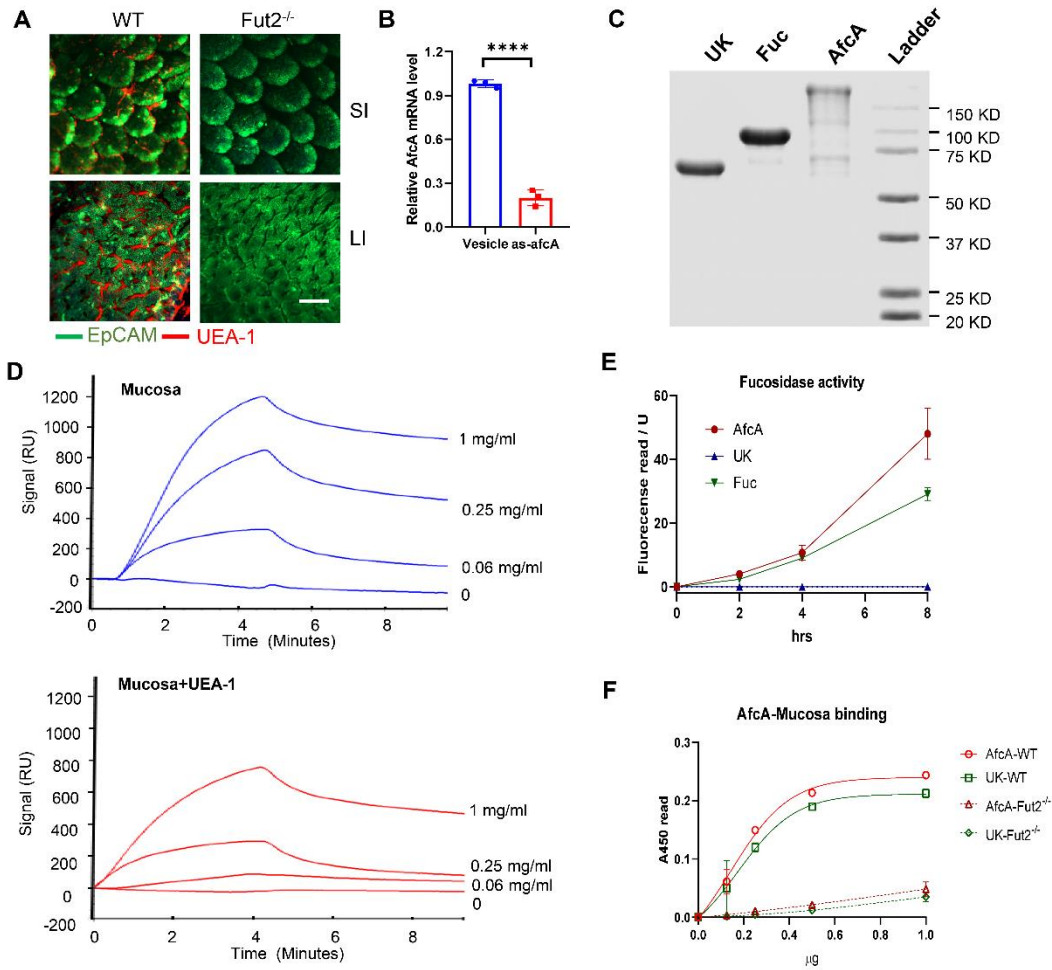


Figure S5 Fucosidase AfcA enhances adhesion and colonization of *Bifidobacterium* in the gut. Related to Figure 5.

(A) Whole mount microscopy of UEA-1 (red) and EpCAM (green) staining of intestine in WT mice or Fut2^{-/-} mice. Scale bar, 50 µm.

(B) Real-time PCR analysis of *afcA* expression in *B. bifidum* transfected with a specific antisense RNA directed against *afcA* (as-afcA).

(C) Purified full-length or truncated AfcA from *B. bifidum* were separated by SDS-PAGE and visualized by staining with Coomassie brilliant blue. The molecular mass standard is shown on the right.

(D) The surface plasmon resonance (SPR) assay was performed to determine different concentration of AfcA recombinant protein binding to mucosa in the presence (Bottom) or absence (Top) of UEA-1. The signal output is directly related to changes in binding capacity on the sensor surface.

(E) Fucosidase activities of purified full-length or truncated AfcA are measured by fluorescence for detecting cleavage of 4-methylumbelliferyl-fucopyranoside substrate.

(F) Binding properties of AfcA full-length or truncated recombinant protein to mucosa from WT mice or *Fut2*^{-/-} mice, as determined by ELISA. Mucosa-coated wells were incubated with 0.125 to 1 µg recombinant protein. Binding was detected with an anti-His antibody.

Data are representative of 2-3 independent experiments. Mean ± SEM; n = 5; ****p < 0.0001.

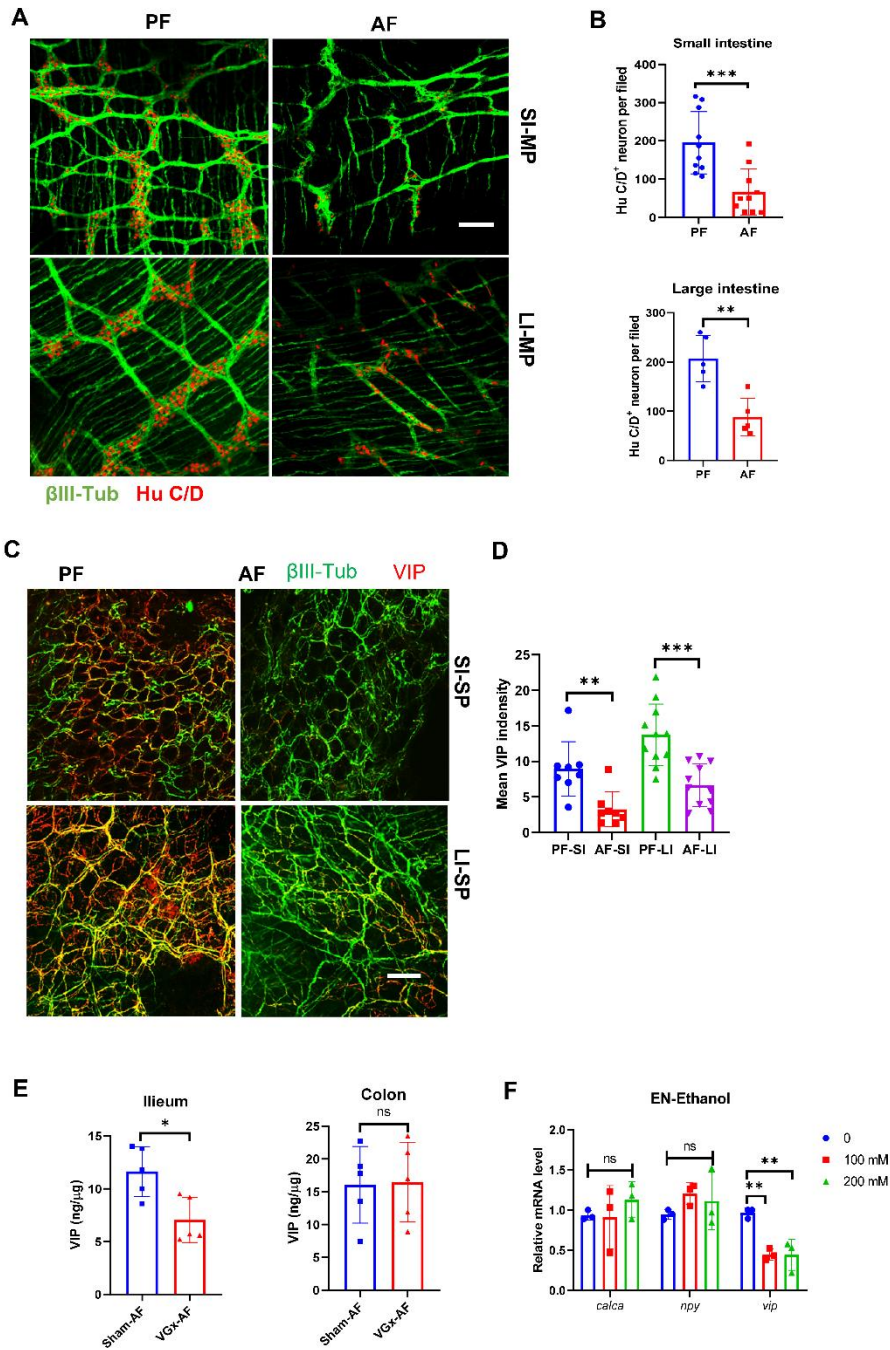


Figure S6 chronic alcohol consumption reduces VIPergic enteric neurons. Related to Figure 6.

(A-B) Mice were fed the paired diet (PF) or alcohol diet (AF) for 50 days. Representative images (A) and quantification (B) of Hu C/D⁺ neurons from small and large intestinal myenteric plexus of

mice. Representative data of 2 independent experiments are shown as mean \pm SEM, n=5; **p < 0.01, ***p < 0.001. Scale bar, 50 μ m.

(C-D) Representative whole mount images (C) and image quantification (D) of VIP neurons by markers staining with β III-Tub (green), VIP (red), and DAPI (blue) in the submucosal plexus of the small and large intestine in mice fed the paired or alcohol diet. Scale bar, 50 μ m.

(E) EIA measurement of concentration of VIP in the ileum and colon of Sham mice or VGx mice after alcohol feeding.

(F) Enteric neurons from small intestinal myenteric plexus were adapted to cultures for 8 days, then treated with ethanol for 24 h, and the effect on expression of the indicated genes assessed by real-time PCR. Error bars Mean \pm SEM; n =3-5, **p < 0.01, representative of 2 independent experiments.

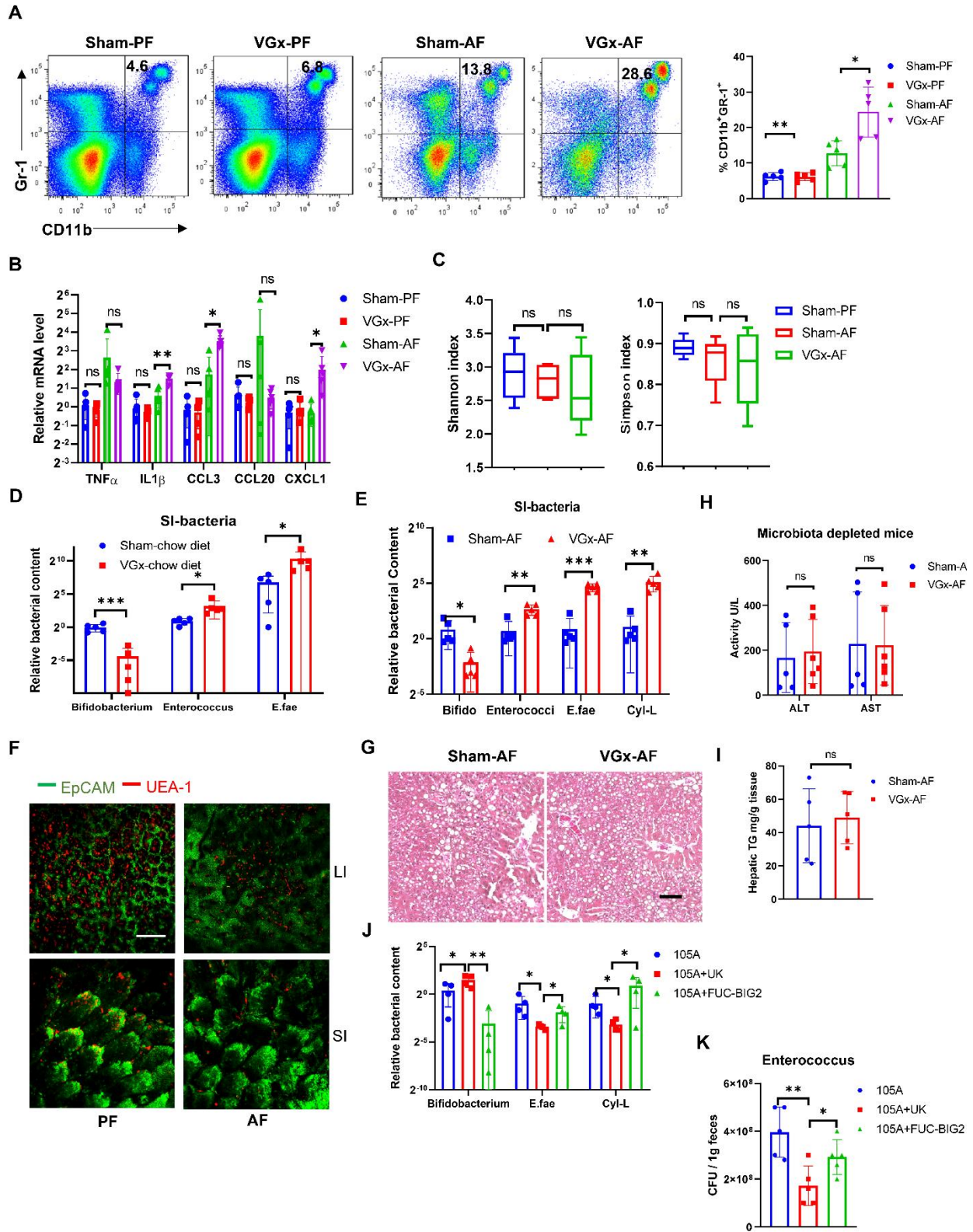


Figure S7 Vagotomy promotes ALD by regulating mucosa-associated bacterial colonization via gut microbiota. Related to Figure 6 and Figure 7.

(A-B) Sham mice or VGx mice were fed the control or alcohol diet and sacrificed 15 days later. Pair feeding (PF); Alcohol feeding (AF).

(A) Representative plots of FACS and summary graphs of the percentage of CD11b⁺Gr-1⁺ myeloid cells in the liver.

(B) Real-time PCR analysis of the relative expression of indicated genes in the liver.

(C) Alpha diversity represented by the Shannon and Simpson index (n=5).

(D-E) Relative levels of *Bifidobacterium*, *Enterococci*, *E. faecalis* (*E.fae*) or cytolysin-producing *E. faecalis* (Cyl-L) in the lumen in chow diet (D) or alcohol diet (E)-fed mice assessed by real-time PCR.

(F) Whole mount microscopy of UEA-1 staining of gut in mice with pair feeding (PF) and alcohol feeding (AF) for 50 days. Scale bar, 50 μ m.

Representative data of 3 independent experiments are shown as mean \pm SEM. *p < 0.05, **p < 0.01, ***p < 0.001, n=5-7.

(G-I) Intestinal decontamination reduces alcohol-induced liver disease in VGx mice. Sham (n=5) and VGx mice (n=5-7) were fed an ethanol diet and treated with antibiotics.

(G) Representative H&E staining of liver sections. Scale bar, 50 μ m.

(H) Plasma level of ALT and AST.

(I) Hepatic triglyceride content.

(J-K) Co-colonization of *B. longum* 105A strain (105A), 105A with the UK domain (105A+UK) or 105A with the Fuc+Big2 domain (105A+Fuc-Big2) and *E. faecalis* in SPF mice. Relative abundance of bacterial genera in fecal samples determined by real-time PCR (J) or total enterococci cfu in the lumen assessed by plating (K).

Representative data of 2 independent experiments are shown as mean \pm SEM. ns indicates not significant. *p < 0.05, **p < 0.01.

Table S1 Primers Related to STAR Methods

Names	Sequences
Bifidobacterium	5'-TCGCGTC(C/T)GGTGTGAAAG-3' 5'-CCACATCCAGC(A/G)TCCAC-3'
E. faecalis	5'-CGCTTCTTTCTCCCGAGT-3' 5'-GCCATGCGGCATAAACTG-3'
Cyl-L	5'-CTGTTGCGGCGACAGCT-3' 5'-CCACCAACCCAGCCACAA-3'
Universal 16S	5'-AAACTCAAAGGAATTGACGG-3' 5'-CTCACRRCACGAGCTGAC-3'
Enterococcus	5'-CCCTTATTGTTAGTTGCCATCATT-3' 5'-ACTCGTTCTTCCCATGT-3'
Fut1	5'-CAAGGAGCTCAGCTATGTGG-3' 5'-GACTGCTCAGGACAGGAAGG-3'
Fut2	5'-ACAGCCAGAAGAGCCATGGC-3' 5'-TAACACCGGGAGACTGATCC-3'
Villin	5'-GCTTGCCACAACCTCCTAAG-3' 5'-CTTGCTTGAAGTAGCTCCGG-3'
GMD	5'-GAGAAAGGTACGAGGTCCAT-3' 5'-TTTTCACTAGGCAGGTGCTGT-3'
GFT	5'-GTGGACGGACGGGCG-3' 5'-CAGAAATGGCTTGTCCCGC-3'
Fx	5'-GGAAGTAGCTCTTGGGCTGG-3' 5'-TTTGGGCTGCATCCGTCAG-3'
FcsK	5'-GGATATCATGACCCACCGGC-3' 5'-TGTCCAAAACCAAGCCCTGT-3'
AfcA-RT	5'-ACCGTGAAGTACAACAAGGAC-3' 5'-TTGTACCACAGCCAGTCGTC-3'
RpoB	5'-AAGGATTACACCTACTCGGCG-3' 5'-TCGCCATGAACACGGTCTG-3'
as-afcA	5'-GAAGACACAAGTCGCCGACGG-3' 5'-TAATACGACTCACTATAGGGACGGCCGACGCAGGTAGTC
pET28	5'-TGAGATCCGGCTGCTAACAAAG-3' 5'-GCCGCTGCTGTGATGATGATG-3' 5'-ATCATCATCACAGCAGCGGCAAACATAGAGCGATGTCATC

AfcA-EX	5'-TTGTTAGCAGCCGGATCTCAGGCGGAGCGCTTGCGGCGAATC-3'
UK-EX	5'-ATCATCATCACAGCAGCGGCAAACATAGAGCGATGTCATC 5'-TTGTTAGCAGCCGGATCTCAATAGGCGTTGAACGAAGCGGC-3'
Fuc-EX	5'-ATCATCATCACAGCAGCGGCGTCATCGCCAGTGTGAGGAC-3' 5'-TTGTTAGCAGCCGGATCTCAGCTCGCCTTCTTCGTGATCGT-3'
pBFS38	5'-TGAGCGGCCGCCCTCAGGTG-3' 5'-CATAGCATCCTTCTTGGGGCCG-3'
pBFS38-Erm	5'-CCCCAAGAAGGATGCTATGAACAAAAATATAAAATATTCTCA-3' 5'-CACCTGAGGGCGGCCGCTCATTTCTCCCGTTAAATAATAG-3'
pBFS38-AfcA	5'-CCCCCAAGAAGGATGCTATGAAACATAGAGCGATGTCATCGCG-3' 5'-CACCTGAGGGCGGCCGCTCAGGCGGAGTGCTTGCGGC-3'
pBFS38-UK	5'-CCGCTTCGTTCAACGCCTATAAGTCCGTCAAGGCCGATACC-3' 5'-ATAGGCGTTGAACGAAGCGG-3'
Enf184-Atto488	5'-CCTCTTTCCAATTGAGTGCA-3'
Bif228-Atto647N	5'-GATAGGACGCGACCCCAT-3'
afcA-Cy3	5'-CCGTGGGCGAGACCAAGAAGA-3'
erm-Atto488	5'-AACACTAGGGTTGCTCTTGCACA-3'
A.muc-fuc	5'-CACTCTTCTCGGAACGCTT-3' 5'-CGTAGAATTCCATGCGCTGC-3'
<hr/>	
B.pse-fuc	5'-CGACGGGTTCCAGATGTACC-3' 5'-CGATGTGCAGAAGTGCAGTC-3'
B.the-fuc	5'-AGCAAGATGAACCTATGATGCA-3' 5'-TTAGCCAATGATTCCCAAGTAG-3'
L.cas-fuc	5'-GTATGGCAACTTGGCAACCG-3' 5'-CATTGCTTAGCGAGTGCAC-3'
T.san-fuc	5'-TAAGGTTTGGCGGTACGCAT-3' 5'-CCGTTGCGTAGATGGCATTG-3'
C-fos	5'-GGGAATGGTGAAGACCGTGTC-3' 5'-GCAGCCATCTTATTCCGTTCCC-3'
Parasutterella	5'-AACGCGAAAAACCTTACCTACC-3' 5'-TGCCCTTTCGTAGCAACTAGTG-3'
Turicibacter	5'-CAGACGGGGACAACGATTGGA-3' 5'-TACGCATCGTCGCCTTGTA-3'
Microbacterium	5'-GAAGGCATCTTCAGCGG-3' 5'-CGTGTCTCAGTCCCAGTGTG-3' 5'-GGTTGTAAACCTCTTTCAS-3'

Rhodococcus	5'-CCTACGARCTCTTTACGC-3'
Enterorhabdus	5'-TCGTAAACCGCTTTCAGCAG-3'
	5'-TAGAGGTTCCGCTTAGGCGG-3'
Brevundimonas	5'-CAGCTAACGCATTAAGCAATC-3'
	5'-CGTTGCTTCGAATTAACCAC-3'
Fut2-AP1-Mut	5'-AATAGCAGAGCCCACAGAGGCTACACAC-3'
	5'-TAGCCTCTGTGGGCTCTGCTATTCCCTCACCCCTGGGCTTTCC-3'
p16337	5'-ACTGTTGGTAAAGCCACCATG-3'
	5'-TCTGTAGAACAAGCTGGCTTC-3'
p16337-Fut2	5'-AAGCCAGCTTGTCTACAGAGTCAGCCATAGGGGGTGAGTG-3'
	5'-ATGGTGGCTTTACCAACAGTGACCCGGAGGAGGCAGTCAAAG-3'
VIP	5'-TTGGCAAACGAATCAGCAGC-3'
	5'-CATTTGCTTTCTGAGGCGGG-3'
<hr/>	
Calca	5'- CCTTTCCTGGTTGTCAGCATCTTG-3'
	5'-CTGGGCTGCTTTCCAAGATTGAC-3'
Npy	5'-TGGCCAGATACTACTCCGCT-3'
	5'-TTGTTCTGGGGCGTTTTTCT-3'
β -actin	5'-ACGGCCAGGTCATCACTATTC-3'
	5'-AGGAAGGCTGGAAAAGAGCC-3'
TNF- α	5'-TCTATGGCCCAGACCCTCAC-3'
	5'-GACGGCAGAGAGGAGGTTGA-3'
IL-1 β	5'-GCAACTGTTCTGAACTCAACT-3'
	5'-ATCTTTTGGGGTCCGTCAACT-3'
CCL3	5'-TTCTCTGTACCATGACACTCTGC-3'
	5'-CGTGGAATCTTCCGGCTGTAG-3'
CCL20	5'-GCCTCTCGTACATACAGACGC-3'
	5'-CCAGTTCTGCTTTGGATCAGC-3'
CXCL1	5'-CTGGGATTCACCTCAAGAACATC-3'
	5'-CAGGGTCAAGGCAAGCCTC-3'
